Targeting autophagy by small molecule inhibitors of vacuolar protein sorting 34 (Vps34) improves the sensitivity of breast cancer cells to Sunitinib

Dyczynski, Matheus

2018-07-25

Dyczynski , M , Yu , Y , Otrocka , M , Parpal , S , Braga , T , Henley , A B , Zazzi , H , Lerner , M , Wennerberg , K , Viklund , J , Martinsson , J , Grandér , D , De Milito , A & Pokrovskaja Tamm , K 2018 , ' Targeting autophagy by small molecule inhibitors of vacuolar protein sorting 34 (Vps34) improves the sensitivity of breast cancer cells to Sunitinib ' Cancer Letters , vol. 435 , pp. 32-43 . DOI: 10.1016/j.canlet.2018.07.028

http://hdl.handle.net/10138/238349
https://doi.org/10.1016/j.canlet.2018.07.028

Cancer Letters 435 (2018) 32–43

Contents lists available at ScienceDirect

Cancer Letters

journal homepage: www.elsevier.com/locate/canlet

Original Articles

Targeting autophagy by small molecule inhibitors of vacuolar protein sorting 34 (Vps34) improves the sensitivity of breast cancer cells to Sunitinib

Matheus Dyczynski[a,1], Yasmin Yu[a,b,1], Magdalena Otrocka[c], Santiago Parpal[b], Tiago Braga[b], Aine Brigette Henley[b], Henric Zazzi[d], Mikael Lerner[a], Krister Wennerberg[e], Jenny Viklund[b], Jessica Martinsson[b], Dan Grandér[a,2], Angelo De Milito[a,b,1], Katja Pokrovskaja Tamm[a,*,1]

[a] Department of Oncology-Pathology, Cancer Center Karolinska, Karolinska Institutet, Stockholm, Sweden
[b] Sprint Bioscience, Huddinge, Sweden
[c] Chemical Biology Consortium Sweden, Science for Life Laboratory Stockholm, Department of Medical Biochemistry and Biophysics, Karolinska Institutet, Solna, Sweden
[d] PDC Center for High Performance Computing, KTH, Stockholm, Sweden
[e] Institute for Molecular Medicine Finland, FIMM, University of Helsinki, Helsinki, Finland

ARTICLE INFO

Keywords:
Autophagy
Combination therapy
Erlotinib
Vps34
High-content screening

ABSTRACT

Resistance to chemotherapy is a challenging problem for treatment of cancer patients and autophagy has been shown to mediate development of resistance. In this study we systematically screened a library of 306 known anti-cancer drugs for their ability to induce autophagy using a cell-based assay. 114 of the drugs were classified as autophagy inducers; for 16 drugs, the cytotoxicity was potentiated by siRNA-mediated knock-down of Atg7 and Vps34. These drugs were further evaluated in breast cancer cell lines for autophagy induction, and two tyrosine kinase inhibitors, Sunitinib and Erlotinib, were selected for further studies. For the pharmacological inhibition of autophagy, we have characterized here a novel highly potent selective inhibitor of Vps34, SB02024. SB02024 blocked autophagy *in vitro* and reduced xenograft growth of two breast cancer cell lines, MDA-MB-231 and MCF-7, *in vivo*. Vps34 inhibitor significantly potentiated cytotoxicity of Sunitinib and Erlotinib in MCF-7 and MDA-MB-231 *in vitro* in monolayer cultures and when grown as multicellular spheroids. Our data suggests that inhibition of autophagy significantly improves sensitivity to Sunitinib and Erlotinib and that Vps34 is a promising therapeutic target for combination strategies in breast cancer.

1. Introduction

Development of drug resistance and/or intrinsic failure to respond to drug treatment represent major obstacles in clinical oncology. Macroautophagy (autophagy) represents an important pathway among the several mechanisms adopted by cancer cells to overcome cytotoxicity of anticancer agents [1,2]. Autophagy is a catabolic degradative pathway highly conserved through evolution, with its primary role as a survival process [3]. Organelles (damaged and/or redundant), protein aggregates, mitochondria, lipids, invading pathogens and other cytoplasmic material are engulfed by a double-membrane-surrounded autophagosome which fuses with a lysosome [4]. In the auto-lysosome, the cargo material is degraded by hydrolases and returned to the cytosol to support macromolecular biosynthesis and cellular metabolism. Autophagy is considered to be a protective cellular mechanism against many human pathologies, including cancer, neurodegeneration, inflammation and infectious diseases [5]. Modulation of autophagy is being evaluated as a therapeutic strategy in some pathological

Abbreviations: AKT, Protein kinase B; ATG7, Autophagy-related protein 7; BafA1, Bafilomycin A1; Chk1, Checkpoint kinase 1; CQ, Chloroquine; FGFR, Fibroblast growth factor receptor; GFP, Green fluorescent protein; HCQ, Hydroxychloroquine; HDAC, Histone deacetylase; HER2, Human epidermal growth factor receptor 2; KU, KU-0063794; LC3, Microtubule-associated proteins 1A/1B light chain 3; MCL-1, Induced myeloid leukemia cell differentiation protein 1; MCS, Multicellular spheroids; mTOR, Mechanistic target of Rapamycin; NCOA4, Nuclear receptor coactivator 4; p62, Sequestosome-1/p62; PI3K, Phosphatidylinositol-3-kinase; PI3P, Phosphatidylinositol 3-phosphate; PROPPIN, β-propellers that bind polyphosphoinositides; Vps34, Vacuolar protein sorting 34

* Corresponding author. Department of Oncology-Pathology, Cancer Center Karolinska, Karolinska Institutet, Karolinska University Hospital, 17176, Stockholm, Sweden.
E-mail address: katja.pokrovskaja@ki.se (K. Pokrovskaja Tamm).
[1] #These authors equally contributed to this work.
[2] Author deceased.

https://doi.org/10.1016/j.canlet.2018.07.028
Received 4 May 2018; Received in revised form 10 July 2018; Accepted 21 July 2018

conditions [6]. Interestingly, the role of autophagy in cancer biology seems to be context-dependent. Cell-autonomous autophagy may play a protective role by maintaining cellular homeostasis and reducing damage from oxidative stress. In many advanced cancers, autophagy supports tumor growth by promoting adaptation to environmental and metabolic stress [1,7]. Recently, an important pro-tumorigenic role has also been demonstrated for non-cell autonomous (or microenvironmental) autophagy [8].

In several *in vitro* and *in vivo* models, autophagy was found to contribute to the development of resistance to chemo- and radiotherapy [9]. These preclinical findings have prompted clinical trials testing the addition of anti-malaria drugs chloroquine (CQ) or hydroxychloroquine (HCQ) to enhance the efficacy of different cancer treatments [7,10]. For example, high levels of autophagy are associated with the development of resistance to BRAF inhibitors [11] and the combination of vemurafenib with CQ showed important clinical benefits [12]. Recent studies have also indicated that autophagy is involved in breast cancer biology [13,14] and in the development of therapy resistance in breast cancer [15,16].

Vps34 is a class III phosphatidylinositol-3-kinase (PI3K) catalyzing the phosphorylation of phosphatidylinositol at the 3′ position of the inositol ring to produce phosphatidylinositol 3-phosphate (PI3P). The lipid kinase activity of VPS34 is fundamental for the biogenesis of autophagosomes since proteins containing a PI3P-binding domain (like FYVE, PROPPIN or PX domain) are recruited to the nascent phagophore and contribute to the maturation of autophagosomes [17]. Vps34 promotes the development of breast cancer [18,19] and has recently been identified as a target to inhibit autophagy [20–22].

In this study, we performed a high-content screening using a library of anticancer drugs currently used preclinically and clinically and identified drugs inducing autophagy. We further assessed whether pharmacological or RNAi-mediated autophagy inhibition potentiated the cytotoxic effects of autophagy-inducing drugs, among them Sunitinib and Erlotinib. Moreover, we describe for the first time a novel, highly potent and selective small molecule inhibitor of Vps34, SB02024, that efficiently inhibited autophagy and cell viability of breast cancer cells *in vitro* and *in vivo*, and when combined with Sunitinib, enhanced its cytotoxic effects in both conventional cell cultures and in multicellular spheroids of breast cancer cell lines.

2. Materials and methods

2.1. Cell culture

HOS cells stably expressing GFP-LC3 (a kind gift from Gerald McInerney, Karolinska Institutet) were cultured in DMEM containing 10% fetal bovine serum (FBS) [23]. MDA-MB-231 cells and MDA-MB-231 cells stably expressing GFP-LC3 were grown in DMEM supplemented with 10% FBS and 1% non-essential amino acids (NEAA). MCF-7 cells were cultured in RMPI-1640 medium containing 10% FBS, 1% NEAA, 1 mM sodium pyruvate and 10 μg/mL insulin. MCF-7 cells stably expressing RLuc-LC3wt or RLuc-LC3G120A (a kind gift from Marja Jäättelä, Danish Cancer Society) [24] were cultured in RPMI-1640 medium with 10% FBS. H1299 cells were maintained in RPMI-1640 medium with 20% FBS. All cell lines were cultured with antibiotics. All products were purchased from Thermo Scientific. MDA-MB-231, MCF-7 and H1299 were purchased from the American Tissue Culture Collection (ATCC). MDA-MB-231 expressing GFP-LC3 were kindly provided by from Yangqing Xu (Harvard Medical School, Boston, MA). Cell lines were tested using the ATCC cell line authentication service and routinely tested for Mycoplasma. All cell lines were maintained at 37 °C with 5% CO_2.

2.2. GFP-2xFYVE expressing H1299 cells

H1299 cells were infected with a lentiviral vector encoding a GFP-2xFYVE construct (Vectalys) consisting of GFP protein tagged with two repeats of a sequence corresponding to the FYVE domain of the Hrs protein at the Ct end and separated by a linker. Infection was carried out according to manufacturer's protocol at 0.3–0.6 multiplicity of infection (MOI) followed by puromycin selection and FACS sorting.

2.3. Chemicals and compound library

Bafilomycin A1 (BafA1, #B1793) and Chloroquine (CQ, #C6628) were purchased from Sigma. Ku-0063794 (KU, #S1226), Sunitinib (#S1042), Erlotinib (#S1023) and PIK-III (#S7683) were purchased from Selleckchem. The compound library was obtained from High Throughput Biomedicine (HTB) unit at the Institute for Molecular Medicine Finland (FIMM) and contained U.S. Food and Drug Administration/European Medicines Agency (FDA/EMA)-approved oncology drugs (n = 129), as well as emerging investigational and preclinical compounds (n = 177) covering a wide range of molecular targets (Supplementary Table 1). Compounds were received diluted in dimethyl sulfoxide (DMSO) or water at different concentrations depending on their biological activity. For screening purposes, compound stocks were dispensed from Labcyte 384 LDV plates to V-bottom Greiner plates using an Echo 555 acoustic liquid handler (LabCyte) and diluted in cell culture medium.

2.4. High-content screen of autophagy modulation

HOS cells stably expressing GFP-LC3 were plated at a density of 1000 cells/well in 384-well imager quality black clear bottom plates (BD Falcon) using a Multidrop dispenser (Thermo Scientific). The following day, the compound library was dispensed using the Bravo liquid handling system (Agilent). DMSO or 10 μM KU (positive control) were manually added using a multichannel pipette. Cells were treated in duplicate for 4, 8 or 16 h and 10 nM BafA1 was added for the last hour of treatment [25]. Cells were fixed and stained in 4% paraformaldehyde (PFA) with 25 mg/mL Hoechst 33342 (Sigma, #B2261) followed by washing steps. Images (4/well) were captured on Operetta® High Content Imaging System (Perkin Elmer) using a 20X LWD objective in widefield fluorescence mode in 2 fluorescent channels (Em.360–340/Ex.410–480, Hoechst 3334; Em.360–340/Ex.410–480 and Em.460–490/Ex.500–550 for GFP-LC3) and further analysed using Columbus 2.4 analysis software (PerkinElmer). "*Find Nuclei Building Block*" algorithm was applied to identify Hoechst-33342-labeled nuclei and was then used as a seeding point to identify cytoplasm with "*Find Cytoplasm Building Block*". "*Find Spots Building Block*" was applied to identify GFP aggregates for measurement of LC3 incorporation into autophagosomes/autolysosomes. "*Calculate Intensity Properties Building blocks*" was used to determine cell number and GFP-LC3 puncta/cell. The results were exported as mean values/well. Z′ factor values for each plate for different quantification parameters were calculated using Columbus tertiary analysis. Data were visualized using Spotfire software.

For high content fluorescent microscopy beyond the screening, images (6/well) were captured on ImageXpress Micro (Molecular Devices) and analysed using the MetaXpress software (Molecular Devices). "Transfluor" algorithm was applied to identify Hoechst-33342-labeled nuclei and GFP-LC3 puncta area/cell. Results were exported as mean values/well. Data were visualized using GraphPad (Prism).

2.5. Western blotting

Cell pellets were lysed in lysis buffer (50 mM Tris, 150 mM NaCl, 1 mM EDTA, 1% Triton X-100, 1% glycerol, adjusted to pH 8) supplemented with protease and phosphatase inhibitors (Roche) and 1 mM DTT. Protein concentration was determined by Pierce BCA Protein Assay (Thermo Scientific) and equal amount of proteins were loaded on

4–12% Bis-Tris gels (NuPAGE, Thermo Scientific). After transfer, PVDF membranes were blocked in 5% milk in TBST (0.05% Tween-20) and incubated with primary antibodies overnight at 4 °C. Membranes were incubated for 1 h at room temperature with appropriate HRP-conjugated secondary antibodies and binding was revealed using the ECL system (#34577, Thermo Scientific). Antibodies against p62 (#5114) and LC3B (#2775) were purchased from Cell Signalling Technologies, NCOA4 (#sc-20011) from Santa Cruz Biotechnologies, Vps34 (#GTX129528) from GeneTex, β-actin (#A5441) from Sigma, goat anti-rabbit HRP (#A16110) and goat anti-mouse HRP (#A16078) from Thermo Scientific.

2.6. Cell viability assays

HOS cells were plated and simultaneously reverse-transfected using HiPerFect transfection reagent (Qiagen) with non-targeting 25 nM siScramble (siSCR; D-001810-10-20, Dharmacon) or 25 nM siRNA targeting *ATG7* (L-020112-00-0005, Dharmacon) and *VPS34* (L-005250-00-0005, Dharmacon) specified as siATG7/siVPS34. The day after transfection, drugs were added, and viability was measured 48 and 72 h after treatment using the CellTiter-Glo assay (Promega).

MDA-MB-231 (5×10^3 cells/well) and MCF-7 (2.5×10^3 cells/well) cells were plated in 96-well plates and treated with compounds the following day. Viability was measured 72 h after treatment using the acid phosphatase (APH) assay [26] for MDA-MB-231 or the CellTiter-Glo assay for MCF-7 following the manufacturer's instructions.

2.7. Clonogenic assay

Cells were plated at a density of 500 cells/well in 6-well plates and treated with compounds the following day. Three days after treatment medium was replaced with drug-free medium. After growing for another three days, colonies were fixed in 4% PFA and stained with 0.05% Crystal violet. The ImageJ-plugin "ColonyArea" optimized for quantitative analysis of foci formation assays was used as previously reported [27].

2.8. Formation and viability of multicellular spheroids

Multicellular spheroids (MCS) from MDA-MB-231 and MCF-7 cells were prepared as previously described [28]. Briefly, cells were plated in 100 µL medium in round bottom, ultra-low attachment 96-well plates (Costar, #7007). MCS from MCF-7 cells (1×10^4 cells/well) were obtained by leaving the plate at RT for 30 min to sediment cells before moving into the incubator. MDA-MB-231 cells (5×10^3 cells/well) were resuspended in medium supplemented with 0.24 µg/µL Geltrex™ LDEV-Free Reduced Growth Factor Basement Membrane Matrix (#A1413202, Thermo Scientific) and centrifuged for 15 min at 1000 × g at 4 °C. The medium of four-days-old MCS was replaced with fresh medium containing different combinations of drugs and compounds. Cell viability was assessed three days after treatment using the CellTiter Glo 3D assay (Promega).

2.9. In vivo experiments

MDA-MB-231 cells (5×10^6) resuspended in PBS with Matrigel (1:1) were subcutaneously implanted in the lower abdomen of female SCID-Beige mice (5–6 weeks of age). MCF-7 cells (1×10^7) resuspended in PBS with Matrigel (1:1) were inoculated in the mammary fat pad of NOD/SCID mice. Mice were randomized into groups of 5–10 mice/group. SB02024 was administered orally once daily. Control animals received the vehicle. Body weight and clinical symptoms were recorded daily. Tumor volume was measured three times a week using a digital caliper (V = 0.5 × length × width [2]). Experiments with MDA-MB-231 and MCF-7 xenografts were performed by GVK Bio (Hyderabad, India) and Crown Bioscience (Beijing, China), respectively. Procedures involving the care and use of animals were approved by the Vivo Bio-Tech animal ethics committee (VB/IAEC/01/2016/129/Mice/SCID) and IACUC committee of CrownBio (AN-1702-013-736).

2.10. Determination of off-target kinase activity and compound K_d

SB02024 and PIK-III were tested on the KINOMEscan™ platform (DiscoverX, Fremont, CA) as previously described [29]. SB02024 and PIK-III were tested at 1 µM concentration in the ScanEDGE™ kinase assay panel containing 97 kinases. SB02024 was further tested 1 µM concentration in the ScanMAX™ kinase assay including a larger set of 468 kinases. Inhibitor binding constants (K_d values) for PIK-III and SB02024 were determined for 9 relevant kinases (PIK3C3, PIK3CA, PIK3CB, PIK3CD, PIK3CG, mTOR, PIK3C2B, PIK3C2G, PIKFYVE) with a top screening concentration of 30 µM.

2.11. Statistical analysis

Statistical analysis was performed with GraphPad (Prism). Comparisons between groups were performed using a two-tailed unpaired *t*-test. P-values of < 0.05 (*), < 0.01 (**), < 0.001 (***) were determined to be statistically significant. Sample size (n) refers to biological replicates unless stated otherwise.

Primary screening of the drugs was calculated with ANOVA [30] using the R software package (https://www.R-project.org/). Drugs that had a significantly higher activity ($p < 0.05$) when treated with BafA1 in comparison to cells without BafA1 were classified as inducers of autophagy, whereas drugs that did not have such a significantly higher activity in the presence of BafA1 in comparison to cells without BafA1, but still had a significantly higher activity ($p < 0.05$) in comparison with the negative control, were classified as blockers.

3. Results

3.1. Modulation of autophagy by anticancer drugs: primary and secondary screening

A major aim of this study was to identify autophagy-inducing anticancer drugs whose cytotoxic activity can be potentiated by inhibiting autophagy. To measure the effect of known anti-cancer drugs on the autophagic turnover we employed a high content screening assay using the osteosarcoma cell line HOS stably expressing GFP-LC3 fusion protein (Fig. 1A). Upon activation of autophagy, the lipidated form of LC3 protein (LC3-II) accumulates in autophagosomes which are visible as GFP + puncta. Inhibition of the autophagic flux by BafA1 blocks the acidification of lysosomes and therefore the final degradation of GFP-LC3, thus further increasing the number of GFP-LC3+ puncta. Ku-0063794 (KU), a mTOR inhibitor previously described to activate autophagy [31] served as a positive control. The images were quantified and the number, as well as the area, of fluorescent puncta per cell were calculated (Supplementary Fig. S1A). Although the autophagy-modulating activity of drugs may be cell line and/or tumor type dependent, these types of cellular systems are easy, robust and have been frequently used for screening purposes. The screening was carried out on a library of anti-cancer drugs and drug candidates routinely used for precision medicine at FIMM [32–34]. An overview of the complete screening procedure is shown in Fig. 1A. Initially, compounds were tested at a 1000-fold dilution of the stock at three time points: 4, 8 and 16 h in the absence or presence of BafA1, which was added 1 h before the fixation and nuclear staining. Fig. 1B shows results obtained after quantification of images acquired after 8 h of incubation with the drugs. The average of GFP-LC3 puncta/cell were normalized to the values obtained with KU as a positive control (100% autophagy induction). Screening quality was overall good as assessed by a Z prime factor of 0.59 ± 0.15. We applied a threshold (mean + 3X SD of the DMSO-treated samples) to identify active molecules. Separate thresholds were

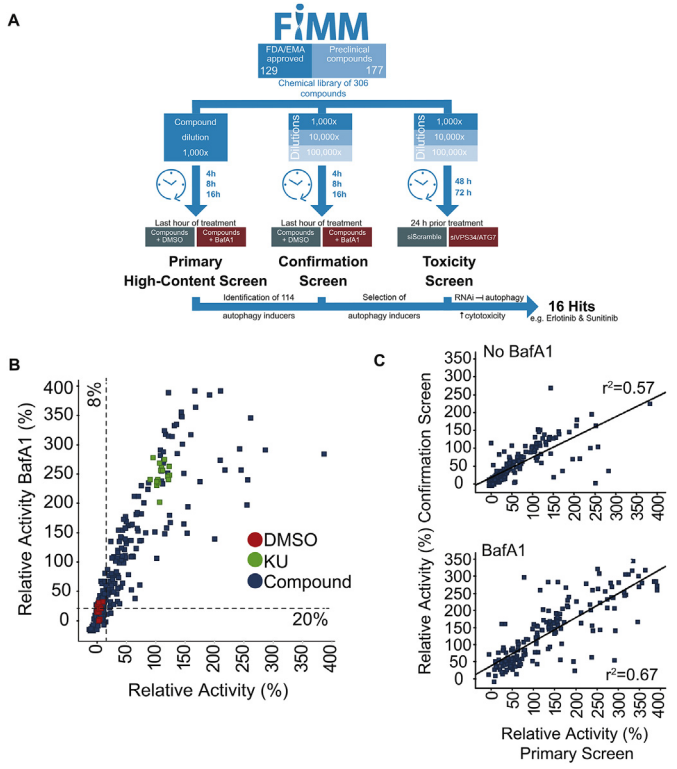

Fig. 1. Screening of anticancer drug library for induction of autophagy. **(A)** Flowchart depicting the screening procedure. Primary and secondary (confirmation) screens of the FIMM oncology collection drug library was performed in HOS osteosarcoma cell line expressing GFP-LC3 using high-content screening fluorescence microscopy. Toxicity screen was conducted in the same cell line where autophagy was inhibited by RNAi with Vps34 and Atg7, using viability assay (Fig. 2). **(B)** Scatter plot of the results of the primary screening. HOS-GFP-LC3 cells were treated with DMSO (red), library compounds (blue), or 10 μM KU-0063794 (KU), used as a positive control (green), for 8 h; 10 nM Bafilomycin A1 (BafA1) was added for the last hour of treatment. The number of GFP + puncta per cell was recorded as described in M&M and set as 0% activity in cells treated with DMSO and as 100% activity in cells treated with KU. The percent of relative activity in the presence of BafA1 (y-axis) was plotted against relative activity in the absence of BafA1 (x-axis). The dashed lines indicate respective thresholds applied for identification of active drugs. **(C)** Correlation of data obtained in primary and confirmation screenings of the drug library (at 1000 fold dilution) tested alone (upper panel) or in the presence of BafA1 (lower panel).

calculated for each time point and for both screening conditions and relatively applied to the sample values measured for drug alone and in presence of BafA1 (Supplementary Fig. S1B). The compound library was then subjected to the confirmation screening performed at three different concentrations (1,000, 10,000 and 100,000-fold stock dilution) and at three time points in the absence or presence of BafA1 in accordance with the primary screening (Supplementary Fig. S1C). The primary screening data correlated well to the data obtained in the confirmation screening (Figs. 1C) with only 8 substances failing to be confirmed.

Drugs were classified as autophagy inducers, autophagy blockers or as negatives (Supplementary Table 1) based on their significant activity ($p < 0.05$) in the presence or absence of BafA1 or in comparison with the negative control, as described earlier. In total 114 drugs, out of 304 in the drug library, were classified as inducers of autophagy. Among known autophagy inducers, we found mTOR, Chk1 and HDAC inhibitors [35], thus, validating our results (Supplementary Table 1).

3.2. Modulation of cell viability by autophagy inhibition: cytotoxicity screening

We next aimed to investigate if inhibition of autophagy would modulate sensitivity to the identified autophagy-inducing drugs. For this purpose, we chose to inhibit *ATG7* and *VPS34*, two autophagy genes crucial for autophagosome formation and maturation. RNAi-mediated knockdown of *ATG7* and *VPS34* (alone or in combination) resulted in significantly reduced expression of the specific mRNA compared to cells treated with siSCR in HOS-GFP-LC3 cells (Fig. 2A). The double knockdown was selected as this condition reduced GFP-LC3 + puncta of both basal and KU-induced autophagy more efficiently (Fig. 2B and C). We assessed cell viability of siRNA-transfected cells treated with the drug library at three different concentrations (Fig. 2D and Supplementary Fig. S2A). For each drug, we calculated the ratio of viability between siATG7/VPS34 versus siSCR, with a ratio < 1 indicating increased cytotoxicity in cells with inhibited autophagy. As a result, we found that among the 114 drugs classified as autophagy inducers, 16 drugs had increased cytotoxic activity upon genetic inhibition of autophagy (threshold < 0.8) (Fig. 2D).

3.3. Sunitinib and Erlotinib modulate autophagic flux in breast cancer cell lines

Human breast carcinomas are particularly sensitive to inhibition of autophagy [14,36,37] and preclinical, as well as clinical, evidence suggests that autophagy inhibition may improve response to treatments in breast cancer [16,38]. Therefore, we evaluated if the drugs – inducers of autophagy - identified in the toxicity screening would also induce autophagy in breast cancer cells. Six out of the 16 inducers identified in HOS-GFP-LC3 cells also induced autophagy in the MDA-MB-231 GFP-LC3 cells. This was evident by an increased number of GFP-LC3 + puncta in the presence of BafA1 as compared to drug treatment alone (Fig. 3A). Among these, Sunitinib and Erlotinib have shown a promising pre-clinical but a limited efficacy in the treatment of breast cancer patients [39,40]. Therefore, these drugs were chosen for further investigation with the aim to explore whether the combination with autophagy inhibition would improve their efficacy. Titration of Sunitinib in MDA-MB-231-GFP-LC3 revealed an induction of autophagy and autophagic flux at low, clinically relevant concentrations (Fig. 3B, Supplementary Fig. S3A). Titration of Erlotinib increased autophagic flux as well, although not to the same extent as Sunitinib (Supplementary Fig. S3B). Interestingly, Sunitinib seemed to inhibit autophagic flux at the highest concentration tested (20 μM) indicated by a no further increase of GFP-LC3 puncta in the presence of BafA1 (Fig. 3B). This was confirmed in another breast cancer cell line, MCF-7-GFP-LC3, which showed similar effects of Sunitinib on autophagic flux (Fig. 3C). This probably reflects the ability of Sunitinib to localize to the lysosomes and to inhibit lysosomal degradation at higher concentrations [41]. We have chosen a concentration of 3 μM for further experiments. The specificity of autophagy induction was confirmed using MCF-7 cells ectopically expressing a GFP-LC3 G120A, a mutant LC3 unable to localize to the autophagosomes [24] and therefore failing to accumulate GFP-positive foci (Supplementary Fig. S3C, D). Next, induction of autophagic flux by 3 μM Sunitinib was analysed using autophagy markers LC3B, NCOA4 and p62 [21,25] by Western blotting (Fig. 3D and E). Sunitinib induced accumulation of LC3B-II protein levels, as well as of NCOA4 and p62 in the presence of BafA1 in MCF-7 cells (Fig. 3E) while these effects were not pronounced in MDA-MB-231 cells (Fig. 3D). This is likely due to high basal autophagic rate in these cells as compared to MCF-7 (compare LC3B-II levels and LC3-I vs. LC3B-II levels in Fig. 3D and E). Neither p62 nor NCOA4 was significantly changed in MDA-MB-231 cells at 6 h of Sunitinib treatment while NCOA4 levels clearly elevated after 24 h of Sunitinib treatment (Fig. 3D and E). This could be due to lysosomal targeting by Sunitinib shown by previous reports [24] or an autophagy-independent

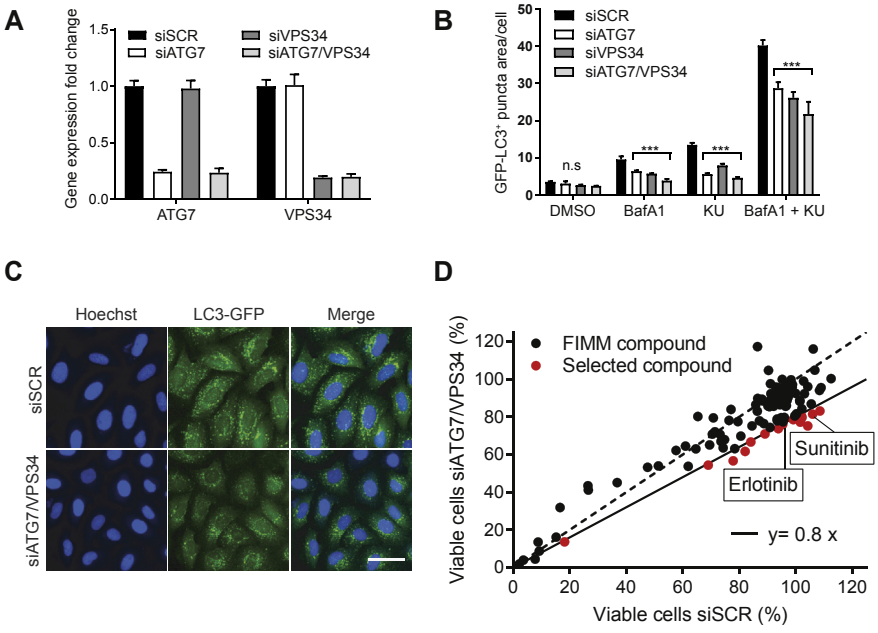

Fig. 2. Modulation of cell viability by autophagy inhibition: cytotoxicity screening.
HOS-GFP-LC3 cells were transfected with 25 nM siRNA targeting ATG7, VPS34, ATG7/VPS34 or non-targeting siRNA Scramble (siSCR) and treated with the drugs from the FIMM library. **(A)** Gene expression levels of ATG7 and VPS34 measured by qRT-PCR 48 h after transfection with indicated siRNA. Means + SD of triplicates are shown. **(B)** Quantification of GFP + puncta area after treatment with DMSO, 10 nM Bafilomycin A1 (BafA1), 10 μM KU-0063794 (KU) or a combination of both BafA1 + KU (n = 3). Means + SD are shown, ***P < 0.001, two-tailed unpaired *t*-test. **(C)** Fluorescence microscopy images of cells transfected with either siSCR or siATG7/VPS34 and treated with BafA1 + KU. Hoechst nuclear stain (blue), LC3-GFP (green), or merge of both channels are shown. Scale bar: 50 μm. **(D)** Scatter plot of the results of the cytotoxicity screen. siRNA-transfected cells were treated with DMSO or drugs that induced autophagy in the secondary screen for 72 h. Viability was measured using CellTiter Glo assay. Compounds selected for further validation are denoted in red. The percentage of viable cells in siSCR transfected (x-axis) versus siATG7/VPS34 transfected (y-axis) cells are plotted.

regulation of NCOA4 expression [41,42]. Thus, the extent of autophagy induction by Sunitinib appears to be dose- and cell line-dependent.

3.4. Novel small molecule Vps34 inhibitor SB02024 inhibits autophagic flux

To evaluate the potential application of pharmacological autophagy inhibition in combination treatment of breast cancer we explored targeting Vps34. A number of small molecular inhibitors of Vps34 have previously been published, including PIK-III [21,43]. Here, we present the biological activities of SB02024, a novel, potent and selective Vps34 inhibitor whose chemical and pharmacological properties will be described elsewhere (manuscript in preparation) in comparison to PIK-III. SB02024 was selected from a series of compounds with high biochemical potency inhibiting Vps34, which in turn was shown to have the ability to inhibit autophagy in cellular systems (patents WO/2017/140841 and WO/2017/140843). SB02024 is a highly potent Vps34 inhibitor (K_d = 1 nM) and more than 1000 times selective towards the other PI3K isoenzymes (Table 1) as well as highly selective at 1 μM in the DiscoveRx ScanMax panel of 468 kinases (Supplementary Fig. S4A). Comparing to the previously published Vps34 inhibitor PIK-III (K_d = 0.3 nM), we found that SB02024 has a similar selectivity profile for the PI3K isoenzymes, except for PIK3CG, where SB02024 is 40 times more selective (Table 1). Also, SB02024 is more selective than PIK-III in the ScanEDGE kinase panel (Supplementary Fig. S4B). Similarly to PIK-III [21], SB02024 is an ATP competitive inhibitor and binds in the active site of Vps34 thus inhibiting its catalytic function.

Considering the crucial role of Vps34 in the autophagic machinery, we examined the effect of Vps34 inhibition on PI3P production and autophagy. With FYVE being a PI3P-specific lipid-binding domain, we generated H1299 cells stably expressing a GFP-2xFYVE construct to measure the effect of Vps34 inhibition on PI3P distribution (Fig. 4A and B). RNAi with VPS34 dramatically reduced GFP-2xFYVE puncta under basal conditions or when autophagy was induced by either Ku or amino acid starvation (Supplementary Fig. S4C). Consistent with the RNAi knockdown, pharmacological treatment with SB02024 also reduced the number of GFP-2xFYVE puncta in a dose-dependent manner (IC_{50} = 14 nM) (Fig. 4A and B). Inhibition of Vps34 activity using small molecular weight compounds is expected to block autophagy, as previously reported for PIK-III [21]. We, therefore, investigated if the induction of autophagy by mTOR inhibitor KU can be prevented by Vps34 inhibition with SB02024. In HOS-GFP-LC3 cells, SB02024 inhibited KU-induced GFP-LC3+ puncta formation in a dose-dependent manner (Fig. 4C and D). To gain further insight into the impact of SB02024 on autophagy, we analysed the expression of autophagy markers and their degradation rate in MDA-MB-231 and MCF-7 cells treated with increasing concentrations of SB02024 for 24 h in the presence or absence of BafA1 during the last 2 h of treatment (Fig. 4E and F, respectively). We observed that SB02024 induced a dose-dependent increase in levels of NCOA4 and p62 which are not further modulated by BafA1, suggesting that Vps34 inhibition blocks the turnover of autophagy substrates (Fig. 4E and F). In line with this observation, total levels of LC3-II were slightly increased by SB02024 and the turnover of LC3-II was also completely inhibited (Fig. 4E and F). We did not observe any changes in the expression of the Vps34 protein upon treatment with SB02024 (Fig. 4E and F). Furthermore, electron microscopy analysis of MDA-MB-231 cells treated with Vps34 inhibitors PIK-III and SB02024 revealed the presence of large empty vacuoles or vacuoles filled with smaller vesicles and undigested electron-dense material. These structures likely represent swollen endolysosomal vesicles, as previously described in cells lacking Vps34 (Supplementary Fig. S4D) [44].

3.5. VPS34 inhibitor SB02024 inhibits tumor growth in vivo

Recently, several small molecule Vps34 inhibitors have been described [43]. Yet, *in vivo* anticancer activity has only been reported for the compound SAR-405, which failed to reduce tumor growth in a xenograft model of human head and neck cancer [45]. Following the results obtained *in vitro*, we investigated the effects of SB02024 treatment *in vivo* in mice bearing MDA-MB-231 or MCF-7 xenografts (Fig. 4G and H, respectively). Mice were treated for 30 (MDA-MB-231) or 21 (MCF-7) days with SB02024 (20 and 50 mg/kg) given by oral gavage. SB02024 treatment reduced significantly tumor growth at the dose of 50 mg/kg at termination in both tumor models (Fig. 4G and H). In line with this, tumor weight was significantly reduced following 50 mg/kg SB02024 treatment for MDA-MB-231 (Supplementary Fig. S4E). This was not the case for the MCF-7 xenografts, and one possible explanation is the lower number of animal (5/group) in the MCF-7 study and the occurrence of one death one day before termination in the group treated with 50 mg/kg of SB02024. Importantly, SB02024 treatment did not affect body weight and treated animals did not show clinical

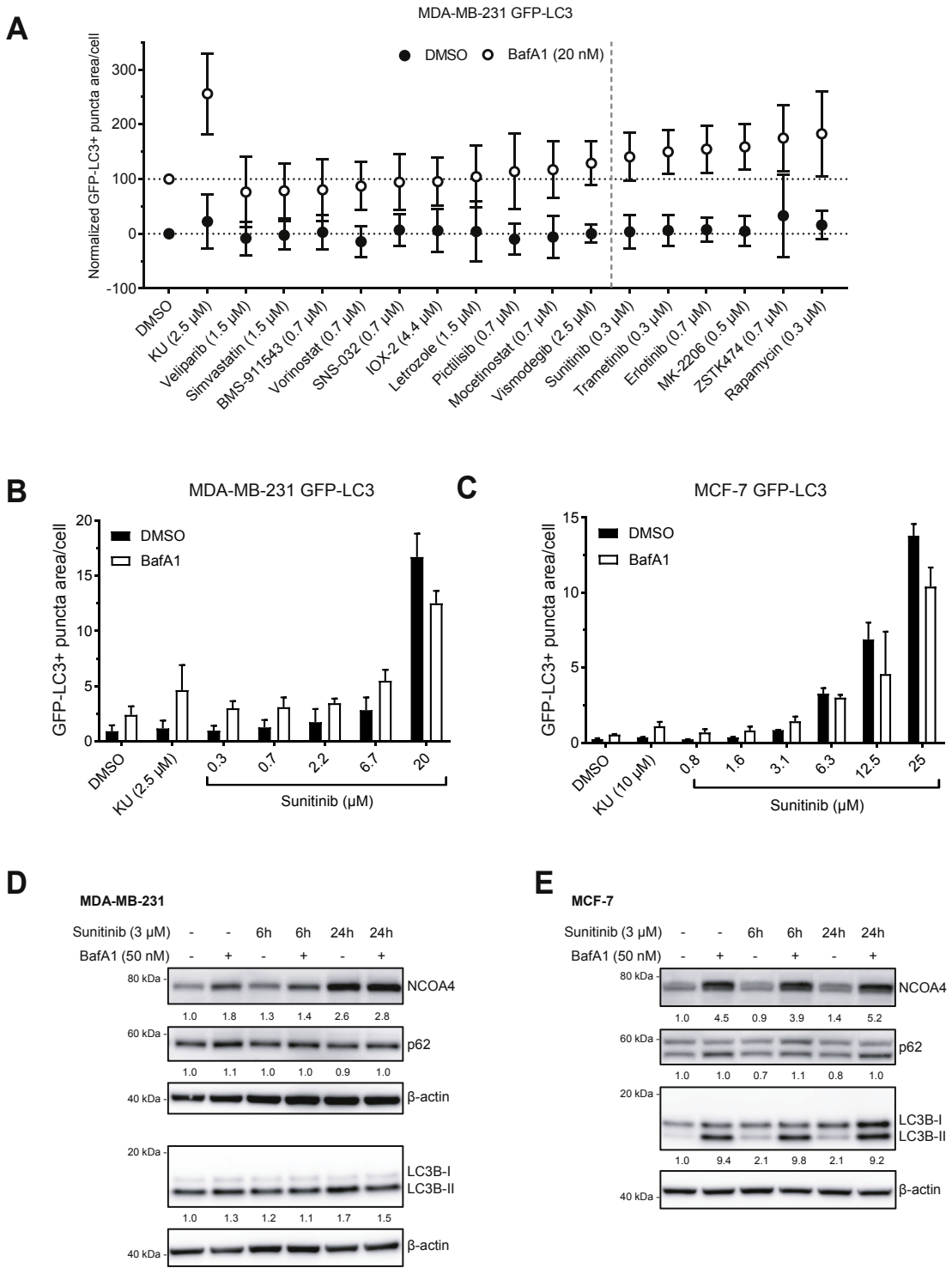

Fig. 3. Sunitinib modulates autophagic flux in breast cancer cell lines.
(A) MDA-MB-231 cells expressing GFP-LC3 were treated with DMSO, KU-0063794 (KU) as a control, or specified drugs at indicated concentrations for 6 h; 20 nM Bafilomycin A1 (BafA1) was added for the last 2 h of treatment. GFP + puncta area was quantified as described in M&M. Six compounds on the right side of the grey dotted line were identified as autophagy inducers. Means ± SD of triplicates are shown. **(B, C)** Quantification of GFP + puncta area of MDA-MB-231 (B) and MCF-7 (C) expressing GFP-LC3 treated with DMSO, KU or Sunitinib at indicated concentrations for 6 h; 20 nM BafA1 was added for the last 2 h of treatment. Means + SD of triplicates are shown. **(D, E)** MDA-MB-231 (D) and MCF-7 (E) cells were treated with 3 μM Sunitinib or DMSO for 6 and 24 h; 50 nM BafA1 was added for the last 2 h of incubation. Autophagic flux was measured by assessing levels of NCOA4, p62, and LC3B-II using Western blotting. β-actin was used as a loading control. A representative blot of two independent experiments is shown. Quantification using Image J is indicated below images and represents the mean of two independent experiments. Sample loading on upper and lower membrane originated from the same protein lysate.

Table 1
Selectivity profile of SB02024 and PIK-III. K_d values are reported in μM and were determined using KINOMEscan™ assay.

Protein	SB02024	PIK-III
PIK3C3	0.0011	0.0003
PIK3CA	4.5505	4.3264
PIK3CB	1.2693	6.3159
PIK3CD	12.137	5.1468
PIK3CG	8.025	0.2021
mTOR	1.0199	3.1168
PIK3C2B	10.894	7.0849
PIK3C2G	3.2005	3.6645
PIKFYVE	> 30	ND

symptoms of toxicity (Supplementary Fig. S4F). This data pointed at the *in vivo* antitumor efficacy of SB02024 treatment.

3.6. Vps34 inhibitors increase the sensitivity of MDA-MB-231 and MCF-7 cells to tyrosine kinase inhibitors

Since inhibition of autophagy can increase the cytotoxic activity of several anticancer therapeutic agents, including tyrosine kinase inhibitors (TKI) [10,46], we further investigated whether treatment with the Vps34 inhibitors SB02024 and PIK-III would increase the sensitivity of MDA-MB-231 and MCF-7 cells to Sunitinib and Erlotinib. In these experiments, CQ was used in parallel as a reference. Firstly, the IC_{50} of Sunitinib for MDA-MB-231 (IC_{50} = 4.8 μM ± 0.7) and for MCF-7 (5.2 μM ± 0.5) was established (Fig. 5A and B). While both cell lines were similarly sensitive to Sunitinib (Fig. 5A and B), none of them was sensitive to Erlotinib, even at the highest soluble concentration of 10 μM [47] (Supplementary Fig. 5A and B). Notably, MCF-7 cells were more sensitive to both Vps34 inhibitors as compared to MDA-MB-231 cells (Fig. 5A and B). We then assessed the effect of combination treatment in both cell lines using IC_{20} concentrations of SB02024, PIK-III and CQ. Addition of either Vps34 inhibitor to Sunitinib significantly decreased cell viability in both cell lines (Fig. 5C and D). However, CQ had a significant effect on cell viability only in MCF-7 cells when combined with Sunitinib (Fig. 5D). While the addition of Vps34 inhibitors or CQ did not sensitize MDA-MB-231 cells to Erlotinib (Supplementary Fig. S5C), the three compounds enhanced the effect of Erlotinib in MCF-7 cells (Supplementary Fig. S5D). Using the clonogenic assay, we further assessed the efficacy of the combination treatment. For this assay, only MCF-7 cells were used as MDA-MB-231 cells did not form distinct colonies. Strikingly, both Vps34 inhibitors, as well as CQ, significantly potentiated the efficacy of Sunitinib or Erlotinib in reducing clonogenic cell survival (Fig. 5E and F and Supplementary Fig. S5E, F).

Finally, we examined whether these drug combinations would be similarly effective in MDA-MB-231 and MCF-7 cells grown as multicellular spheroids (MCS). We chose to do these experiments with Sunitinib only as both breast cancer cell lines were highly resistant to Erlotinib. Cells grown as MCS were previously reported to activate autophagic flux [48,49] as well as partially recapitulate therapy resistance, so-called multicellular resistance [50,51]. Autophagy induction in MCS as compared to monolayer cultures was monitored using Western blot analysis and revealed a decrease in the autophagic substrate NCOA4 and p62 in the MDA-MB-231, while LC3B-II was increased in the presence of BafA1 in MCF-7 MCS, suggesting, although differential, an autophagy induction in either cell line when grown as MCS (Supplementary Fig. S6A, B). In line with data in Fig. 4, SB02024 inhibited autophagic flux in both monolayer cultures and MCS in either cell line although to a different extent (Supplementary Fig. S6A, B). In MDA-MB-231 MCS, combined treatment with Sunitinib and PIK-III significantly decreased relative cell viability as compared to the Sunitinib treatment alone (Fig. 5G). In MCF-7 MCS, the combination of either SB02024 or PIK-III significantly decreased relative cell viability as compared to Sunitinib alone (Fig. 5H). Interestingly, CQ did not enhance the cytotoxicity of Sunitinib in either of the cell lines grown as MCS. Taken together, the data provide compelling evidence that autophagy inhibition by small molecule inhibitors of Vps34 increases the cytotoxic effects of Sunitinib and Erlotinib as summarised in Fig. 5I.

4. Discussion

In this study, we performed a high-content screening to monitor autophagy induction by anti-cancer drugs and focused on two tyrosine kinase inhibitors, Sunitinib and Erlotinib. We found that Sunitinib and Erlotinib induced autophagy in our screening system as well as in breast cancer cell lines. Furthermore, inhibition of Vps34 could potentiate the cytotoxic effect of these drugs. Also, we report a novel Vps34 inhibitor, namely SB02024, that was able to decrease tumor growth *in vivo* indicating its potential to be developed into a drug for anti-cancer treatment.

We addressed the question of which anti-cancer drugs can induce autophagy in cancer cells. Being fully aware of the limitations of the screening system, such as cell-type specificity and *in vitro* conditions, we have tested a library of anti-cancer drugs in a high content phenotypic screen for autophagy induction to identify more than 1/3 of these drugs being able to induce autophagy. This approach has been used before in a screen of the Institute of Chemistry and Cell Biology (ICCB) library of bioactive compounds and the National Cancer Institute (NCI) mechanistic set library [52]. Our screen of the FIMM drug library, on the other hand, provides data better applicable for translational research: this comprehensive drug library contains most of the clinical and preclinical anti-cancer drugs in physiologically relevant concentrations [32]. We also used a genetic approach to inhibit autophagy in the same screening system to identify drugs whose efficacy was increased by autophagy inhibition. The siRNA-mediated knockdown of *ATG7* and *VPS34* might be suboptimal for autophagy inhibition due to transient nature of RNAi approach, the dynamic nature of autophagy [53] or to the interaction between autophagy and intracellular siRNA delivery [54]. Thus, the number of drugs confirmed to induce a cytoprotective autophagy might be underestimated. Using this approach, we identified two tyrosine kinase inhibitors that we further investigated in combination with autophagy inhibition in cellular models of breast cancer. For this purpose, we inhibited autophagy pharmacologically, using highly specific small molecule inhibitors of Vps34, SB02024 and PIK-III. Several studies have previously demonstrated that induction of autophagy may represent a mechanism for drug resistance [14,15,55]. Indeed, autophagy, as a conserved cellular response to stress, can be a powerful protector against cell-damaging drugs [56]. Also novel targeted therapies, similarly to established cytotoxic drugs, induce multiple resistance mechanisms, including induction of autophagy, and therefore may be inefficient against cancer as a monotherapy [1,56]. Induction of autophagy as an intrinsic property of some targeted therapies may thus be one of the reasons for ineffective clinical trials. For example, the two tyrosine kinase inhibitors that we focused on, Sunitinib and Erlotinib, have shown poor clinical efficacy in breast cancer patients [57,58]. Initially, Sunitinib showed promising results in phase II clinical trials [59] but failed to prolong survival in phase III trials in metastatic and triple-negative breast cancer [60–62]. This prompted us to assess whether autophagy induction might contribute to this lack of a prolonged response. Indeed, in this study, a combination with Vps34 inhibitors significantly increased the sensitivity of breast cancer cells to Sunitinib. Moreover, while these cells were initially very resistant to Erlotinib alone, Vps34 inhibition could overcome this resistance. Further animal studies will allow concluding whether autophagy inhibition can improve the anti-cancer properties of these tyrosine kinase inhibitors for the treatment of breast cancer.

Another important question that we have not addressed in this study is the mechanism of autophagy induction by the tyrosine kinase

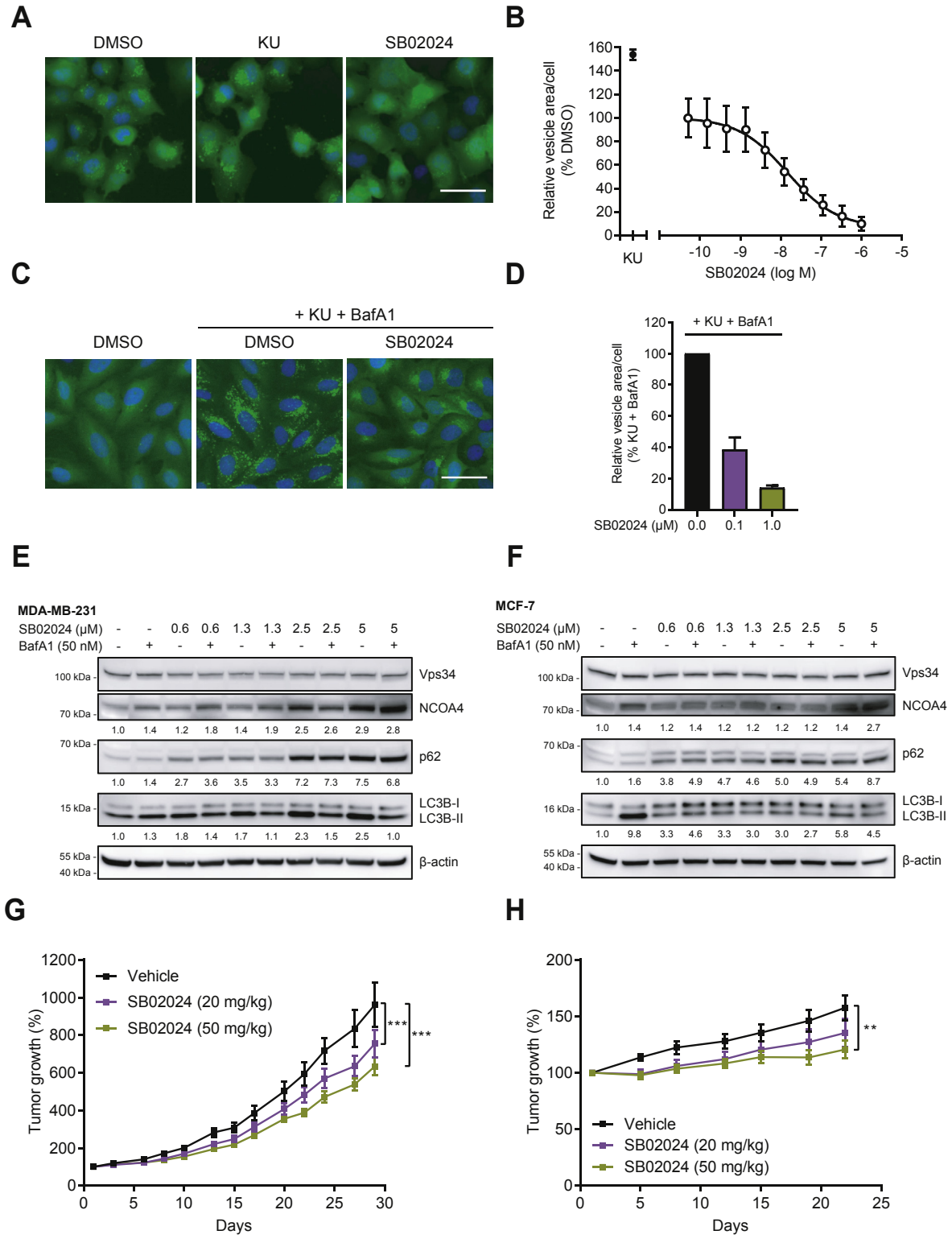

Fig. 4. Vps34 inhibitor SB02024 blocks autophagic flux in vitro and decreases tumor growth of breast cancer xenografts. (A) Fluorescence microscopy images of GFP + puncta area of H1299 cells expressing GFP-2XFYVE treated for 6 h with DMSO, 0,5 μM KU-0063794 (KU) or 0,7 μM SB02024. Scale bar: 50 μm. **(B)** Quantification of the experiment in (A). Values were normalized to DMSO control. Means ± SD of three independent experiments are shown. **(C)** Fluorescence microscopy images of GFP + puncta area of HOS cells expressing GFP-LC3 treated either with DMSO alone or with the combination of 10 μM KU and 10 nM BafA1 in the presence or absence of 1,1 μM SB02024. Scale bar: 50 μm. **(D)** Quantification of the experiment in (C). Values were normalized to the combination of DMSO + KU + BafA1. Means ± SD of three independent experiments are shown. MDA-MB-231 **(E)** and MCF-7 **(F)** cells were treated with DMSO or SB02024 at indicated concentrations for 24 h 50 nM BafA1 was added for the last 2 h of treatment. The effect on autophagic flux was measured by assessing levels of Vps34, NCOA4, p62, and LC3B-II using Western blotting. β-actin was used as a loading control. A representative blot of three independent experiments is shown. Quantification of the band intensity using Image J is indicated below. **(G)** Tumor growth of MDA-MB-231 subcutaneous xenografts treated with vehicle or SB02024 (20 mg/kg or 50 mg/kg, daily) for 30 days. Means ± SEM, n = 10. **(H)** Tumor growth of orthotopic MCF-7 xenografts treated with vehicle (n = 6), 20 mg/kg SB02024 (n = 6) or 50 mg/kg SB02024 (n = 5, n = 4 for last measurement) for 21 days. Means ± SEM are shown; *P < 0.05, **P < 0.01, ***P < 0.001; Tukey's multiple comparisons test.

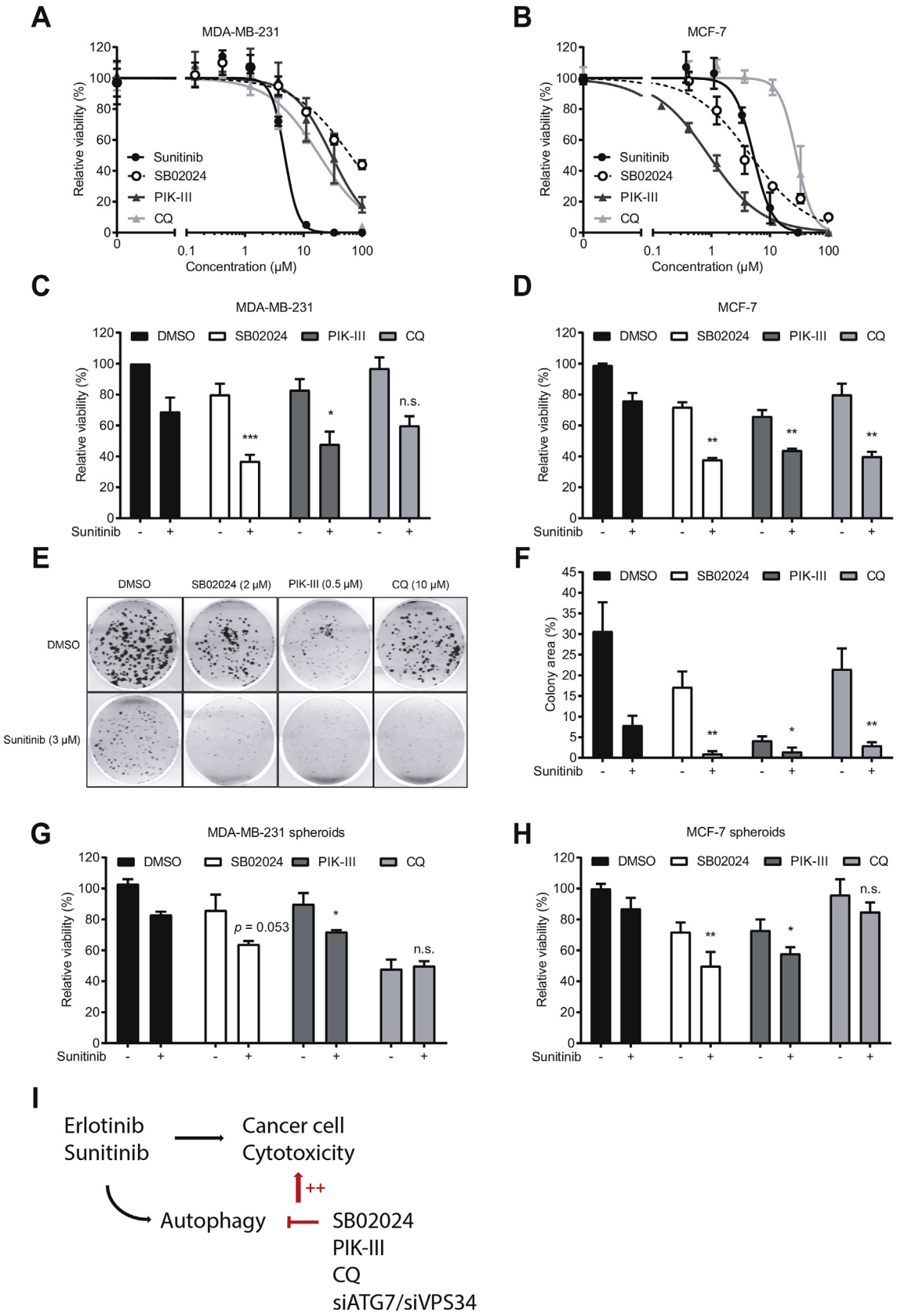

(caption on next page)

Fig. 5. Vps34 inhibitors increase sensitivity of breast cancer cell lines to Sunitinib. **(A)** MDA-MB-231 and **(B)** MCF-7 cells were treated with DMSO, Sunitinib, SB02024, PIK-III or Chloroquine (CQ) at indicated concentrations for 72 h and cell viability was measured as described in M&M. **(C)** MDA-MB-231 cells were treated with 3 μM Sunitinib in combination with either DMSO, 5 μM SB02024, 0.5 μM PIK-III or 5 μM CQ; **(D)** MCF-7 cells were treated with 3 μM Sunitinib in combination with DMSO, 2 μM SB02024, 0.5 μM PIK-III or 15 μM CQ, and cell viability was measured as described in M&M. **(E)** Representative images of MCF-7 cells pre-treated with 3 μM Sunitinib in combination with either DMSO, 2 μM SB02024, 0.5 μM PIK-III or 10 μM CQ to assess clonogenic cell survival as described in M&M. **(F)** Quantification of the experiment in (E). **(G)** MDA-MB-231 and **(H)** MCF-7 cells were cultured as multicellular tumor spheroids and treated for 72 h with 3 μM Sunitinib and either DMSO, 5 μM SB02024, 5 μM PIK-III or 5 μM CQ. Viability was measured using CellTiter Glo 3D assay. For all experiments data was normalized to DMSO treated controls (n = 3). Means and SD are shown, *P < 0.05, **P < 0.01, two-tailed unpaired *t*-test comparing combination treatment versus the most effective compound of the two single compounds. **(I)** Simplified scheme depicting the enhancing effects of autophagy inhibition on Sunitinib and Erlotinib treatment.

inhibitors. Activated tyrosine-kinases support tumor cell growth and survival via several downstream signalling pathways including PI3K/AKT/mTOR pathway. Thus, inhibition of tyrosine kinases will inevitably result in the inhibition of mTOR, which consequently leads to the induction of autophagy [56].

It has been shown that the lysosomal sequestration of Sunitinib may result in the permeabilization of the lysosomal membrane leading to cell death [63,64]. Notably, combination treatments with lysosomal inhibitors have been reported to increase the sensitivity to Sunitinib in several cancer types [41,65]. Another mechanism involving modulation of the anti-apoptotic protein MCL-1 and, again, of the mTOR protein by Sunitinib has also been described to alter autophagic flux [66]. Further studies will be necessary to dissect the exact mechanisms of autophagy activation by each of the tyrosine kinase inhibitors to use this knowledge for the development of novel combination therapies.

Similar to our study, combinations of Vps34 inhibitor with other anti-cancer drugs have been assessed. For example, Vps34 inhibitor SAR405 was able to increase sensitivity to cisplatin of human urothelial carcinoma [67] and head and neck cancer cell lines [68] while a dual FGFR inhibitor also targeting Vps34 increased cisplatin sensitivity of bladder cancer cells [69]. Also, genetic inhibition of Vps34 increased the sensitivity of HER + breast cancer cell lines to class I PI3K or HER2 inhibitors [70]. Collectively, these and our findings strongly support Vps34 as a target in anti-cancer treatment.

Conventional two dimensional (2D) cell culture systems are often poorly predictive of drug efficacy, as we and others have shown [71,72]. Indeed, the growth of tumor cells as MCS better mimics the architecture of tumors and more closely reproduces the heterogeneity of tumor tissue in terms of phenotypic and metabolic features [51,73], which have a crucial impact on therapeutic efficacy [51,72,74,75]. Moreover, cells grown in 3D encounter metabolic stress that in turn may stimulate autophagy, as it was shown in different cancer models [48,49]. Remarkably, even in MCS, being as a rule more resistant to drug treatments, the addition of Vps34 inhibitors potentiated the cytotoxic effect of Sunitinib. This model system also clearly showed that the potent additive effects of CQ in the monolayer culture (based on viability and colony formation assays) are diminished in MCS, most likely due to hypoxia and acidosis characterizing MCS and low activity of CQ in these conditions [75]. Interestingly, there is another aspect of targeting Vps34 in conjunction with Sunitinib. Apart from induction of autophagy, hypoxia may represent an important mechanism mediating resistance to Sunitinib [58,76]. Thus, targeting hypoxia was shown to increase the therapeutic efficacy of Sunitinib *in vivo* [77]. At the same time, targeting Vps34 has been recently shown to inhibit oxygen consumption rate [69,78], raising the possibility that Vps34 inhibition may decrease *in vivo* hypoxia and contribute to improving Sunitinib sensitivity. This further strengthens the notion that using Vps34 inhibitors in combination with targeted tyrosine kinase inhibitor-based therapy, and particularly Sunitinib, can overcome resistance and emphasizes their value in cancer treatment.

Acknowledgments

We would like to thank Marja Jäättelä for kindly providing us the MCF-7 LC3-GFP wild-type and MCF-& LC3-GFPG120A cell lines, Gerald McInerney for kindly providing us the HOS-GFP-LC3 cell line, Lars Hammarström for chemistry support and Kjell Hultenby for support with electron microscopy.

Professor Dan Grandér, who was the grant holder and the senior author of this project at the Department of Oncology & Pathology, passed away in October 2017. The authors are deeply sorrowed by his tragic death and dedicate this study to his memory.

Financial support

This work was supported by Cancerfonden, CF (Grant N 170207) (to D.G. and K.P.) and Konung Gustav V:s jubileumsfond (Grant N 174122) (to D.G. and K.P.). M.D. was supported by Karolinska Institutet's Doctoral grant (KID), Sweden (2415-12-225). Y.Y. was supported by the Swedish Foundation for Strategic Research (Grant ID16-0034). Y.Y., S.P., T.B., A.H., J.V., J.M. and A.D.M. were financially supported by Sprint Bioscience AB, Huddinge, Sweden.

Conflicts of interest

Y.Y., S.P., T.B., A.H., J.V. and A.D.M. are employees of Sprint Bioscience AB. J.M. is a founder of Sprint Bioscience AB. S.P., T.B., J.V., J.M., K.P.T. and A.D.M. are shareholders of Sprint Bioscience AB.

Appendix A. Supplementary data

Supplementary data related to this article can be found at https://doi.org/10.1016/j.canlet.2018.07.028.

References

[1] L. Galluzzi, F. Pietrocola, J.M. Bravo-San Pedro, R.K. Amaravadi, E.H. Baehrecke, F. Cecconi, P. Codogno, J. Debnath, D.A. Gewirtz, V. Karantza, A. Kimmelman, S. Kumar, et al., Autophagy in malignant transformation and cancer progression, EMBO J. 34 (2015) 856–880.
[2] V.W. Rebecca, R.K. Amaravadi, Emerging strategies to effectively target autophagy in cancer, Oncogene 35 (2016) 1–11.
[3] J.J. Lum, R.J. DeBerardinis, C.B. Thompson, Autophagy in metazoans: cell survival in the land of plenty, Nat. Rev. Mol. Cell Biol. 6 (2005) 439–448.
[4] N. Mizushima, T. Yoshimori, Y. Ohsumi, The role of Atg proteins in autophagosome formation, Annu. Rev. Cell Dev. Biol. 27 (2011) 107–132.
[5] A.M.K. Choi, S.W. Ryter, B. Levine, Autophagy in human health and disease, N. Engl. J. Med. 368 (2013) 651–662.
[6] E. Morel, M. Mehrpour, J. Botti, N. Dupont, A. Hamaï, A.C. Nascimbeni, P. Codogno, Autophagy: a druggable process, Annu. Rev. Pharmacol. Toxicol. 57 (2017) 375–398.
[7] J.M.M. Levy, C.G. Towers, A. Thorburn, Targeting autophagy in cancer, Nat. Rev. Canc. 17 (2017) 528–542.
[8] N.S. Katheder, R. Khezri, F. O'Farrell, S.W. Schultz, A. Jain, M.K.O. Schink, T.A. Theodossiou, T. Johansen, G. Juhász, D. Bilder, A. Brech, H. Stenmark, et al., Microenvironmental autophagy promotes tumour growth, Nature 541 (2017) 417–420.
[9] R. Amaravadi, A.C. Kimmelman, E. White, Recent insights into the function of autophagy in cancer, Genes Dev. 30 (2016) 1913–1930.
[10] C. Chude, R. Amaravadi, Targeting autophagy in cancer: update on clinical trials and novel inhibitors, Int. J. Mol. Sci. 18 (2017) 1279.
[11] X.H. Ma, S.F. Piao, S. Dey, Q. McAfee, G. Karakousis, J. Villanueva, L.S. Hart, S. Levi, J. Hu, G. Zhang, R. Lazova, V. Klump, et al., Targeting ER stress-induced autophagy overcomes BRAF inhibitor resistance in melanoma, J. Clin. Invest. 124 (2014) 1406–1417.
[12] J.M.M. Levy, J.C. Thompson, A.M. Griesinger, V. Amani, A.M. Donson, D.K. Birks, M.J. Morgan, D.M. Mirsky, M.H. Handler, N.K. Foreman, A. Thorburn, Autophagy inhibition improves chemosensitivity in BRAFV600E brain tumors, Canc. Discov. 4 (2014) 773–780.

[13] P. Maycotte, C.M. Gearheart, R. Barnard, S. Aryal, J.M.M. Levy, S.P. Fosmire, R.J. Hansen, M.J. Morgan, C.C. Porter, D.L. Gustafson, A. Thorburn, J.M. Mulcahy Levy, et al., STAT3-mediated autophagy dependence identifies subtypes of breast cancer where autophagy inhibition can be efficacious, Canc. Res. 74 (2014) 2579–2590.
[14] S. Lefort, C. Joffre, Y. Kieffer, A.M. Givel, B. Bourachot, G. Zago, I. Bieche, T. Dubois, D. Meseure, A. Vincent-Salomon, J. Camonis, F. Mechta-Grigoriou, Inhibition of autophagy as a new means of improving chemotherapy efficiency in high-LC3B triple-negative breast cancers, Autophagy 10 (2014) 2122–2142.
[15] W. Yang, S.R. Hosford, N.A. Traphagen, K. Shee, E. Demidenko, S. Liu, T.W. Miller, Autophagy promotes escape from phosphatidylinositol 3-kinase inhibition in estrogen receptor–positive breast cancer, FASEB J. 32 (2018) 1222–1235.
[16] K.L. Cook, A. Wärri, D.R. Soto-Pantoja, P.A.G. Clarke, M.I. Cruz, A. Zwart, R. Clarke, Hydroxychloroquine inhibits autophagy to potentiate antiestrogen responsiveness in ER + breast cancer, Clin. Canc. Res. 20 (2014) 3222–3232.
[17] A.C. Nascimbeni, P. Codogno, E. Morel, Phosphatidylinositol-3-phosphate in the regulation of autophagy membrane dynamics, FEBS J. 284 (2017) 1267–1278.
[18] X. Jiang, Y. Bao, H. Liu, X. Kou, Z. Zhang, F. Sun, Z. Qian, Z. Lin, X. Li, X. Liu, L. Jiang, Y. Yang, VPS34 stimulation of p62 phosphorylation for cancer progression, Oncogene 36 (2017) 6850–6862.
[19] D.S. Hirsch, Y. Shen, M. Dokmanovic, W.J. Wu, pp60c-Src phosphorylates and activates vacuolar protein sorting 34 to mediate cellular transformation, Canc. Res. 70 (2010) 5974–5983.
[20] A. Honda, E. Harrington, I. Cornella-Taracido, P. Furet, M.S. Knapp, M. Glick, E. Triantafellow, W.E. Dowdle, D. Wiedershain, W. Maniara, C. Moore, P.M. Finan, et al., Potent, selective, and orally bioavailable inhibitors of VPS34 provide chemical tools to modulate autophagy in vivo, ACS Med. Chem. Lett. 7 (2016) 72–76.
[21] W.E. Dowdle, B. Nyfeler, J. Nagel, R.A. Elling, S. Liu, E. Triantafellow, S. Menon, Z. Wang, A. Honda, G. Pardee, J. Cantwell, C. Luu, et al., Selective VPS34 inhibitor blocks autophagy and uncovers a role for NCOA4 in ferritin degradation and iron homeostasis in vivo, Nat. Cell Biol. 16 (2014) 1069–1079.
[22] B. Ronan, O. Flamand, L. Vescovi, C. Dureuil, L. Durand, F. Fassy, M.-F. Bachelot, A. Lamberton, M. Mathieu, T. Bertrand, J.-P. Marquette, Y. El-Ahmad, et al., A highly potent and selective Vps34 inhibitor alters vesicle trafficking and autophagy, Nat. Chem. Biol. 10 (2014) 1013–1019.
[23] K.E. Eng, M.D. Panas, G.B. Karlsson Hedestam, G.M. McInerney, A novel quantitative flow cytometry-based assay for autophagy, Autophagy 6 (2010) 634–641.
[24] T. Farkas, M. Høyer-Hansen, M. Jäättelä, Identification of novel autophagy regulators by a luciferase-based assay for the kinetics of autophagic flux, Autophagy 5 (2009) 1018–1025.
[25] D.J. Klionsky, K. Abdelmohsen, A. Abe, M.J. Abedin, H. Abeliovich, A.A. Arozena, H. Adachi, C.M. Adams, P.D. Adams, K. Adeli, P.J. Adhihetty, S.G. Adler, et al., Guidelines for the use and interpretation of assays for monitoring autophagy (third edition), Autophagy 12 (2016) 1.
[26] T.-T. Yang, P. Sinai, S.R. Kain, An acid phosphatase assay for quantifying the growth of adherent and nonadherent cells, Anal. Biochem. 241 (1996) 103–108.
[27] C. Guzmán, M. Bagga, A. Kaur, J. Westermarck, D. Abankwa, ColonyArea: an ImageJ plugin to automatically quantify colony formation in clonogenic assays, PLoS One 9 (2014) e92444.
[28] A.P. Andersen, M. Flinck, E.K. Oernbo, N.B. Pedersen, B.M. Viuff, S.F. Pedersen, Roles of acid-extruding ion transporters in regulation of breast cancer cell growth in a 3-dimensional microenvironment, Mol. Canc. 15 (2016) 45.
[29] M.A. Fabian, W.H. Biggs, D.K. Treiber, C.E. Atteridge, M.D. Azimioara, M.G. Benedetti, T.A. Carter, P. Ciceri, P.T. Edeen, M. Floyd, J.M. Ford, M. Galvin, et al., A small molecule–kinase interaction map for clinical kinase inhibitors, Nat. Biotechnol. 23 (2005) 329–336.
[30] J.M. Chambers, A.E. Freeny, R.M. Heiberger, Analysis of variance, Des. Exp. (2017) 145–193.
[31] J.M. García-Martínez, J. Moran, R.G. Clarke, A. Gray, S.C. Cosulich, C.M. Chresta, D.R. Alessi, Ku-0063794 is a specific inhibitor of the mammalian target of rapamycin (mTOR), Biochem. J. 421 (2009) 29–42.
[32] B. Yadav, T. Pemovska, A. Szwajda, E. Kulesskiy, M. Kontro, R. Karjalainen, M.M. Majumder, D. Malani, A. Murumägi, J. Knowles, K. Porkka, C. Heckman, et al., Quantitative scoring of differential drug sensitivity for individually optimized anticancer therapies, Sci. Rep. 4 (2014) 5193.
[33] T. Pemovska, E. Johnson, M. Kontro, G.A. Repasky, J. Chen, P. Wells, C.N. Cronin, M. Mctigue, O. Kallioniemi, K. Porkka, B.W. Murray, K. Wennerberg, Axitinib effectively inhibits BCR-ABL1(T315I) with a distinct binding conformation, Nature 519 (2015) 102–105.
[34] D.J.J. Waugh, Expanding the armamentarium for castrate-resistant prostate cancer, Eur. Urol. 71 (2017) 328–329.
[35] N. Gammoh, D. Lam, C. Puente, I. Ganley, P.A. Marks, X. Jiang, Role of autophagy in histone deacetylase inhibitor-induced apoptotic and nonapoptotic cell death, Proc. Natl. Acad. Sci. U. S. A. 109 (2012) 6561–6565.
[36] N. Lisiak, E. Toton, M. Rybczynska, Autophagy as a potential therapeutic target in breast cancer treatment, Curr. Cancer Drug Targets 18 (2018) 629–639.
[37] P. Maycotte, Targeting autophagy in breast cancer, World J. Clin. Oncol. 5 (2014) 224.
[38] T. Ueno, S. Saji, M. Sugimoto, N. Masuda, K. Kuroi, N. Sato, H. Takei, Y. Yamamoto, S. Ohno, H. Yamashita, K. Hisamatsu, K. Aogi, et al., Clinical significance of the expression of autophagy-associated marker, beclin 1, in breast cancer patients who received neoadjuvant endocrine therapy, BMC Canc. 16 (2016) 230.
[39] A. Elgebaly, A. Menshawy, G. El Ashal, O. Osama, E. Ghanem, A. Omar, A. Negida, Sunitinib alone or in combination with chemotherapy for the treatment of advanced breast cancer: a systematic review and meta-analysis, Breast Dis. 36 (2016) 91–101.
[40] A. Lluch, P. Eroles, J.-A. Perez-Fidalgo, Emerging EGFR antagonists for breast cancer, Expet Opin. Emerg. Drugs 19 (2014) 165–181.
[41] A.-M. Ellegaard, L. Groth-Pedersen, V. Oorschot, J. Klumperman, T. Kirkegaard, J. Nylandsted, M. Jäättelä, Sunitinib and SU11652 inhibit acid sphingomyelinase, destabilize lysosomes, and inhibit multidrug resistance, Mol. Canc. Therapeut. 12 (2013) 2018–2030.
[42] J.M. Goodwin, W.E. Dowdle, R. DeJesus, Z. Wang, P. Bergman, M. Kobylarz, A. Lindeman, R.J. Xavier, G. McAllister, B. Nyfeler, G. Hoffman, L.O. Murphy, Autophagy-independent lysosomal targeting regulated by ULK1/2-FIP200 and ATG9, Cell Rep. 20 (2017) 2341–2356.
[43] B. Pasquier, Autophagy inhibitors, Cell. Mol. Life Sci. 73 (2016) 985–1001.
[44] L.M. Compton, O.C. Ikonomov, D. Sbrissa, P. Garg, A. Shisheva, Active vacuolar H + ATPase and functional cycle of Rab5 are required for the vacuolation defect triggered by PtdIns(3,5)P 2 loss under PIKfyve or Vps34 deficiency, Am. J. Physiol. Physiol. 311 (2016) C366–C377.
[45] J. New, L. Arnold, M. Ananth, S. Alvi, M. Thornton, L. Werner, O. Tawfik, H. Dai, Y. Shnayder, K. Kakarala, T.T. Tsue, D.A. Girod, et al., Secretory autophagy in cancer-associated fibroblasts promotes head and neck cancer progression and offers a novel therapeutic target, Canc. Res. 77 (2017) 6679–6691.
[46] J.M.M. Levy, C.G. Towers, A. Thorburn, Targeting autophagy in cancer, Nat. Rev. Canc. 17 (2017) 528–542.
[47] D. Jawhari, M. Alswisi, M. Ghannam, J Al Halman, Bioequivalence of a new generic formulation of erlotinib hydrochloride 150 mg tablets versus tarceva in healthy volunteers under fasting conditions, J. Bioequiv. Availab. 6 (2014) 119–123.
[48] C. Bingel, E. Koeneke, J. Ridinger, A. Bittmann, M. Sill, H. Peterziel, J.K. Wrobel, I. Rettig, T. Milde, U. Fernekorn, F. Weise, A. Schober, et al., Three-dimensional tumor cell growth stimulates autophagic flux and recapitulates chemotherapy resistance, Cell Death Dis. 8 (2017) e3013.
[49] D. Barbone, C. Follo, N. Echeverry, V.H. Gerbaudo, A. Klabatsa, R. Bueno, E. Felley-Bosco, V.C. Broaddus, Autophagy correlates with the therapeutic responsiveness of malignant pleural mesothelioma in 3D models, PLoS One 10 (2015) e0134825.
[50] H. Kobayashi, S. Man, C.H. Graham, S.J. Kapitain, B.A. Teicher, R.S. Kerbel, Acquired multicellular-mediated resistance to alkylating agents in cancer, Proc. Natl. Acad. Sci. Unit. States Am. 90 (1993) 3294–3298.
[51] J. Friedrich, C. Seidel, R. Ebner, L.A. Kunz-Schughart, Spheroid-based drug screen: considerations and practical approach, Nat. Protoc. 4 (2009) 309–324.
[52] S. Shen, O. Kepp, M. Michaud, I. Martins, H. Minoux, D. Métivier, M.C. Maiuri, R.T. Kroemer, G. Kroemer, Association and dissociation of autophagy, apoptosis and necrosis by systematic chemical study, Oncogene 30 (2011) 4544–4556.
[53] P. Codogno, M. Mehrpour, T. Proikas-Cezanne, Canonical and non-canonical autophagy: variations on a common theme of self-eating? Nat. Rev. Mol. Cell Biol. 13 (2012) 7–12.
[54] R.H. Mo, J.L. Zaro, J.-H.J. Ou, W.-C. Shen, Effects of Lipofectamine 2000/siRNA complexes on autophagy in hepatoma cells, Mol. Biotechnol. 51 (2012) 1–8.
[55] K.L. Cook, A. Wärri, D.R. Soto-Pantoja, P.A. Clarke, M.I. Cruz, A. Zwart, R. Clarke, Hydroxychloroquine inhibits autophagy to potentiate antiestrogen responsiveness in ER + breast cancer, Clin. Canc. Res. 20 (2014) 3222–3232.
[56] X. Sui, R. Chen, Z. Wang, Z. Huang, N. Kong, M. Zhang, W. Han, F. Lou, J. Yang, Q. Zhang, X. Wang, C. He, et al., Autophagy and chemotherapy resistance: a promising therapeutic target for cancer treatment, Cell Death Dis. 4 (2013) e838.
[57] M.N. Dickler, H.S. Rugo, C.A. Eberle, E. Brogi, J.F. Caravelli, K.S. Panageas, J. Boyd, B. Yeh, D.E. Lake, C.T. Dang, T.A. Gilewski, J.F. Bromberg, et al., A phase II trial of erlotinib in combination with bevacizumab in patients with metastatic breast cancer, Clin. Canc. Res. 14 (2008) 7878–7883.
[58] T. Foukakis, J. Lovrot, P. Sandqvist, H. Xie, L.S. Lindstrom, C. Giorgetti, H. Jacobsson, E. Hedayati, J. Bergh, Gene expression profiling of sequential metastatic biopsies for biomarker discovery in breast cancer, Mol. Oncol. 9 (2015) 1384–1391.
[59] H.J. Burstein, A.D. Elias, H.S. Rugo, M.A. Cobleigh, A.C. Wolff, P.D. Eisenberg, M. Lehman, B.J. Adams, C.L. Bello, S.E. DePrimo, C.M. Baum, K.D. Miller, Phase II study of sunitinib malate, an oral multitargeted tyrosine kinase inhibitor, in patients with metastatic breast cancer previously treated with an anthracycline and a taxane, J. Clin. Oncol. 26 (2008) 1810–1816.
[60] J. Bergh, I.M. Bondarenko, M.R. Lichinitser, A. Liljegren, R. Greil, N.L. Voytko, A.N. Makhson, J. Cortes, A. Lortholary, J. Bischoff, A. Chan, S. Delaloge, et al., First-line treatment of advanced breast cancer with sunitinib in combination with docetaxel versus docetaxel alone: results of a prospective, randomized phase III study, J. Clin. Oncol. 30 (2012) 921–929.
[61] G. Curigliano, X. Pivot, J. Cortés, A. Elias, R. Cesari, R. Khosravan, M. Collier, X. Huang, P.E. Cataruozolo, K.A. Kern, A. Goldhirsch, Randomized phase II study of sunitinib versus standard of care for patients with previously treated advanced triple-negative breast cancer, Breast 22 (2013) 650–656.
[62] J. Crown, V. Dieras, E. Staroslawska, D.A. Yardley, N. Davidson, T.D. Bachelot, V.R. Tassell, X. Huang, K.A. Kern, G. Romieu, Phase III trial of sunitinib (SU) in combination with capecitabine (C) versus C in previously treated advanced breast cancer (ABC), J. Clin. Oncol. 28 (2010) LBA1011–LBA1011.
[63] T. Wiedmer, A. Blank, S. Pantasis, L. Normand, R. Bill, P. Krebs, M.P. Tschan, I. Marinoni, A. Perren, Autophagy inhibition improves sunitinib efficacy in pancreatic neuroendocrine tumors via a lysosome-dependent mechanism, Mol. Canc. Therapeut. 16 (2017) molcanther.0136.2017.
[64] K.J. Gotink, H.J. Broxterman, M. Labots, R.R. De Haas, H. Dekker, R.J. Honeywell, M.A. Rudek, L.V. Beerepoot, R.J. Musters, G. Jansen, A.W. Griffioen, Y.G. Assaraf, et al., Lysosomal sequestration of sunitinib: a novel mechanism of drug resistance, Clin. Canc. Res. 17 (2011) 7337–7346.
[65] L. DeVorkin, M. Hattersley, P. Kim, J. Ries, J. Spowart, M.S. Anglesio, S.M. Levi, D.G. Huntsman, R.K. Amaravadi, J.D. Winkler, A.V. Tinker, J.J. Lum, Autophagy inhibition enhances sunitinib efficacy in clear cell ovarian carcinoma, Mol. Canc.

Res. 15 (2017) 250–258.
[66] M. Elgendy, A.K. Abdel-Aziz, S.L. Renne, V. Bornaghi, G. Procopio, M. Colecchia, R. Kanesvaran, C.K. Toh, D. Bossi, I. Pallavicini, J.L. Perez-Gracia, M.D. Lozano, et al., Dual modulation of MCL-1 and mTOR determines the response to sunitinib, J. Clin. Invest. 127 (2017) 153–168.
[67] D. Schlütermann, M.A. Skowron, N. Berleth, P. Böhler, J. Deitersen, F. Stuhldreier, N. Wallot-Hieke, W. Wu, C. Peter, M.J. Hoffmann, G. Niegisch, B. Stork, Targeting urothelial carcinoma cells by combining cisplatin with a specific inhibitor of the autophagy-inducing class III PtdIns3K complex, Urol. Oncol. 36 (2018) 160.e1–160.e13.
[68] J. New, L. Arnold, M. Ananth, S. Alvi, M. Thornton, L. Werner, O. Tawfik, H. Dai, Y. Shnayder, K. Kakarala, T.T. Tsue, D.A. Girod, et al., Secretory autophagy in cancer-associated fibroblasts promotes head and neck cancer progression and offers a novel therapeutic target, Canc. Res. 77 (2017) 6679–6691.
[69] C.-H. Chen, C. Changou, T.-H. Hsieh, Y.-C. Lee, C.-Y. Chu, K.-C. Hsu, H.-C. Wang, Y.-C. Lin, Y.-N. Lo, Y.-R. Liu, J.-P. Liou, Y. Yen, Dual inhibition of PIK3C3 and FGFR as a new therapeutic approach to treat bladder cancer, Clin. Canc. Res. 24 (2018) 1176–1189.
[70] C.D. Young, C.L. Arteaga, R.S. Cook, Dual inhibition of Type I and Type III PI3 kinases increases tumor cell apoptosis in HER2+ breast cancers, Breast Cancer Res. 17 (2015) 148.
[71] J. Friedrich, C. Seidel, R. Ebner, L.A. Kunz-Schughart, Spheroid-based drug screen: considerations and practical approach, Nat. Protoc. 4 (2009) 309–324.
[72] I. Kolosenko, M. Fryknäs, S. Forsberg, P. Johnsson, H. Cheon, E.G. Holvey-Bates, E. Edsbäcker, P. Pellegrini, H. Rassoolzadeh, S. Brnjic, R. Larsson, G.R. Stark, et al., Cell crowding induces interferon regulatory factor 9, which confers resistance to chemotherapeutic drugs, Int. J. Canc. 136 (2015) E51–E61.
[73] L.B. Weiswald, D. Bellet, V. Dangles-Marie, Spherical cancer models in tumor biology, Neoplasia (United States) 17 (2015) 1–15.
[74] F. Hirschhaeuser, H. Menne, C. Dittfeld, J. West, W. Mueller-Klieser, L.A. Kunz-Schughart, Multicellular tumor spheroids: an underestimated tool is catching up again, J. Biotechnol. 148 (2010) 3–15.
[75] P. Pellegrini, A. Strambi, C. Zipoli, M. Hagg-Olofsson, M. Buoncervello, S. Linder, A. De Milito, Acidic extracellular pH neutralizes the autophagy-inhibiting activity of chloroquine: implications for cancer therapies, Autophagy 10 (2014) 562–571.
[76] S. Braga, J. Cardoso, S. Andre, M. Brito, P. Sanchez, L. Orvalho, L. Salgado, S. Dias, J. Pereira-Leal, J. Passos-Coelho, Does hypoxic response mediate primary resistance to sunitinib in untreated locally advanced breast cancer? Curr. Cancer Drug Targets 17 (2016) 62–73.
[77] S. Liu, M.T. Tetzlaff, T. Wang, X. Chen, R. Yang, S.M. Kumar, A. Vultur, P. Li, J.S. Martin, M. Herlyn, R. Amaravadi, B. Li, et al., Hypoxia-activated prodrug enhances therapeutic effect of sunitinib in melanoma, Oncotarget 8 (2017) 115140–115152.
[78] B. Bilanges, S. Alliouachene, W. Pearce, D. Morelli, G. Szabadkai, Y.-L. Chung, G. Chicanne, C. Valet, J.M. Hill, P.J. Voshol, L. Collinson, C. Peddie, et al., Vps34 PI 3-kinase inactivation enhances insulin sensitivity through reprogramming of mitochondrial metabolism, Nat. Commun. 8 (2017) 1804.